

Correlation between permeability and deformational characteristics of the Shirahama sandstone and Inada granite

Korrelation zwischen der Permeabilität und der Deformationseigenschaft von Shirahama Sandstein und Inada Granit

Corrélation entre la perméabilité et les caractéristiques de déformation du grès de Shirahama et du granite d'Inada

M.TAKAHASHI & H.KOIDE, Geological Survey of Japan, A.I.S.T., M.I.T.I., Japan
XUE ZI-QIU, Faculty of Engineering, Hokkaido University, Japan

ABSTRACT: Permeability and volumetric strain were measured of the Shirahama sandstone and Inada granite under hydrostatic and deviatoric stress. A transient pulse method was used to measure the permeability up to nano darcy order. The permeability of the Shirahama sandstone ranged from about 10^{-6} darcy to 2×10^{-5} darcy under isotropic stress. The permeability of the Inada granite ranged from about 3×10^{-8} darcy to 5×10^{-6} darcy under isotropic stress. Permeability was not a simple function of the conventional effective confining pressure (P_c) and internal fluid pressure (P_p). Changes in permeability were found to be proportional to $(P_c - \alpha P_p)$, where the values of α are different for each rocks and for preferred orientation. Nearly threefold increase of permeability occurred in the Shirahama sandstone at axial differential stress of 80MPa as compared with that at the isotropic stress state. Permeability of the Inada granite increased by nearly thirtyfold at 300MPa axial differential stress over the value at the isotropic stress. At the isotropic stress the permeability of rocks is slightly lower after deformation than before deformation. This phenomenon is probably due to the closure of preexisting microcracks. The sample become more dilatant and permeability increases with further increase of the axial differential stress. These observations can be interpreted systematically in terms of differences in the porosity or aperture of the preexisting and stress-induced microcracks during deformation.

RESUME: La perméabilité et déformation volumétrique ont été mesurées au grès de Shirahama et au granite d'Inada en contrainte isotrope et en contrainte déviatrice. La méthode par la pulsation transitoire a été utilisé à la mesure de la perméabilité à l'ordre de nano darcy. La perméabilité du grès Shirahama est du quelque 10^{-6} darcy au 2×10^{-5} darcy en contrainte isotrope. La perméabilité de la granite d'Inada est du quelque 3×10^{-8} darcy au 5×10^{-6} darcy en contrainte isotrope. La perméabilité n'est pas la fonction simple de la pression latérale effective conventionnelle, c'est, la différence de la pression latérale à la pression interstitielle. La perméabilité est la fonction de $(P_c - \alpha P_p)$, où le coefficient α est différent à la roche et à la direction de la granite d'Inada. Presque trois fois augmentation de la perméabilité est provoquée en la grès de Shirahama au déviateur des contraintes 80MPa en comparaison de la perméabilité en contrainte isotrope. La perméabilité de la granite d'Inada s'augmentait presque trente fois au déviateur de contraintes 300MPa en comparaison de la perméabilité en contrainte isotrope. En contrainte isotrope, la perméabilité des roches diminuent après la déformation en comparaison de la perméabilité avant la déformation. Ce phénomène est causé probablement par le clôturation des microfissures préexistantes. L'augmentation du déviateur des contraintes cause la dilatation et l'augmentation de la perméabilité des roches. Ces observations sont explicables systématiquement par la différence de la porosité ou par l'ouverture des microfissures préexistantes et inductives en déformation des roches.

ZUSAMMENFASSUNG: Die Permeabilität und die volumetrische Deformation von Shirahama Sandstein und Inada Granit wurden unter der hydrostatischen und deviatorischen Spannung gemessen. Die transitorische Puls Methode wurde um die Permeabilität bis zum Ordnungszu messen angewandt. Die Permeabilität des Shirahama Sandsteins verändert sich zwischen ungefähr 10^{-6} darcy und 2×10^{-5} darcy unter der hydrostatischen Spannung. Die Permeabilität des Inada Granites verändert sich zwischen ungefähr 3×10^{-8} darcy und 5×10^{-6} darcy unter der hydrostatischen Spannung. Die Permeabilität ist nicht eine einfache funktion von Einschlussdruck (P_c) und innerhalb Poren Flüssigkeitsdruck (P_p). Es wurde deutlich, daß die Veränderung von Permeabilität in einem Verhältnis zu $(P_c - \alpha P_p)$ steht. Wobei sind die Werte von α in jedem Gestein verschieden, und gegenseitig senkrechte Orientierung. Bei der axialen Differenzspannung von 80 MPa war die fast dreifache Zunahme im Shirahama Sandstein festzustellen. Die Permeabilität von Inada Granit nahm fast dreißigfach bei Werten von Null bis 300MPa axiale Differenzspannung zu. Bei der Anfangsspannungshöhe nahm die Permeabilität der Gestein etwas ab. Wahrscheinlich veranlaßte der Abschluß der vorbestehenden des Mikrorisse diese Erscheinung. Die Probe wurde dilatant durch weiterer Zunahme der axialen Differenzspannung, und entsprechend nahm die Permeabilität zu. Diese Beobachtungen können durch der Unterschied in dem Porengehalt oder der Öffnung der Mikrorisse die vorbestehen oder aus die Spannung entstehen, systematisch erklärt werden.

1. Introduction

Fluid flow in the earth's crust plays a major role in some important problems such as earthquake source process, radioactive waste isolation, petroleum accumulation, geothermal activity, and so on. For adequate isolation of radioactive waste, several recent laboratory experiments have been made on the fluid flow through intact, low permeability rocks under elevated temperatures and pressures. Pressure dependence of the transport properties of rocks of great importance. The pressure dependence can be monitored in laboratory tests applied both pore pressure and external isotropic pressure to the sample of rock in a pressure vessel. Many examples of

permeability measurement in laboratory on sandstones, crystalline rocks etc. can be found in the geophysical literatures as well as for the rock engineering practices (Brace 1980).

Kranz et al. (1979) and Bernabe (1986) indicated that permeability is not a function of the simple effective pressure, that is, difference between external confining pressure (P_c) and internal fluid pressure (P_p). They suggested that the permeability of rock is a function of modified effective pressure, that is, the difference between the confining pressure and pore pressure multiplied by a coefficient. Mordecai and Morris (1971) observed changes of permeability in the Darley Dale sandstone prior to fracturing at confining pressures up to 40 MPa. At

the confining pressure of 7 Mpa, the permeability was only 20% lower than that at the atmospheric pressure. At the high pressure of 41 MPa, it actually underwent a 5 % overall increase of permeability before fracture. Zoback and Byerlee(1975) found that at about 80% of the ultimate fracture stress, permeability of Westerly granite increased by a factor of three or four under the 39 MPa effective confining pressure. At 75 MPa effective confining pressure, the permeability of Ottawa sand dropped by a factor of nearly 100 after the peak stress. From above-mentioned results, it is obvious that the permeability of rock is quite dependent to the stress history. In this study, the effect of practical confining pressure and axial differential stress on the permeability is experimentally measured for the Shirahama sandstone and for the anisotropic Inada granite.

2. Permeability measurement with the transient pulse method

In this experiment, permeability of rock was measured with a transient pulse technique similar to the method by Brace et al.(1986). After the pore pressure equilibrated in the sample, the fluid pressure was raised instantaneously by several bars at one side of rock specimen. The pore pressure, then, decreased exponentially with time as fluid flowed through the sample. Permeability is calculated from the decay slope with the next formula.

$$k = m\mu\beta(L/A)(V1+V2)/(V1 \cdot V2)$$

where m is the slope of pressure decay, μ and β are the dynamic viscosity and compressibility of the pore fluid, L and A are the length and cross-sectional area of the sample, and $V1$ and $V2$ are volumes of upstream and downstream reservoirs.

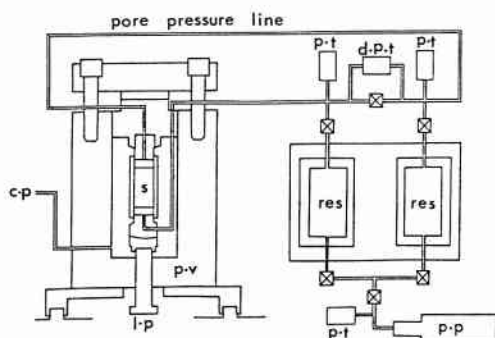


Fig.1 Schematic illustration of the pore pressure system, sample assemblage, and triaxial apparatus. s:specimen p.v:pressure vessel l.p:loading piston p.v:pressure vessel p.t:pressure transducer d.p.t differential pressure transducer res:reservoir for water p.p:pore pressure pump.

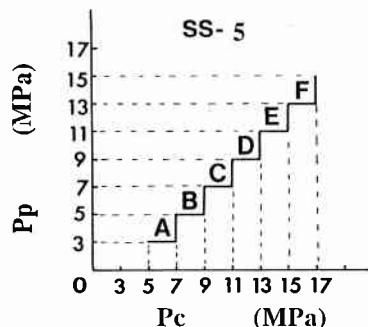


Fig.2 Schematic representation of changes in P_c and P_p of the Shirahama sandstone.

3. Setup of specimens

The specimens of the Shirahama sandstone were cored perpendicular to the bedding plane. Most of granitic rocks are orthotropic in elasticity due to the preferred orientation of pre-existing microcracks. Quarry-men can distinguish a "rift" plane, a "grain" plane, and a "hardway" plane in the order of ease of split. These planes affect the physical properties such as compressional and shear wave velocities, compressive strength, and tensile strength(Kudo et al. 1987). In the Inada granite, the specimen of IGR, IGG, IGH were cored normal to the rift, grain, hardway planes, respectively. These specimens were ground to a cylinder of 30 mm diameter and 60 mm length. Cross type strain gages were fixed to the samples with gauge cement. Fig.1 shows a schematic diagram of the pore pressure system, sample assemblage, and triaxial apparatus used in the experiments. The specimens were jacketed with silicon rubber. The pore fluid was pressurized into specimens through narrow radial and concentric grooves on the surface and pinholes of stainless steel end pieces.

4. Experimental results and discussion

The pressure path in these experiments is indicated

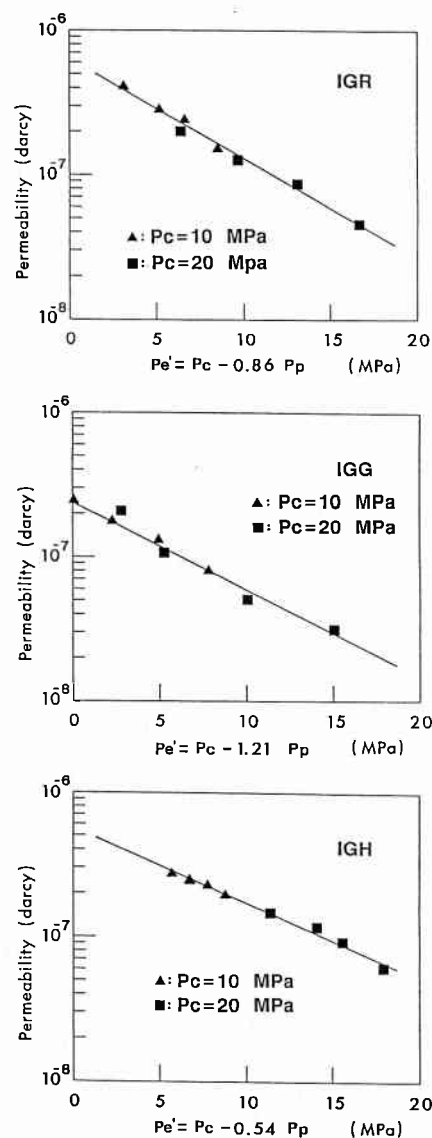


Fig.3 Permeability at modified effective pressure of the Inada granite for different preferred orientations, IGR, IGG, IGH.

schematically in Fig.2. At point(Pc,Pp), α is defined as the slope of the tangent to the curve of constant permeability. In practice, it can be written as $\alpha = -\delta K_p / \delta K_c$, where δK_p and δK_c are the variations of K respectively caused by independent change of Pp or Pc by the same small amount δp (δp is positive during loading cycles and negative during unloading cycles). Bernabe(1986) mentioned that α is strongly dependent on the order in which Pc and Pp were applied to the samples. From their observations, they persisted that α took relatively low values when δK_c was measured before δp , and relatively high values in the other case. In our experiments, δK_c was measured before δK_p . Measured values of α in each pressure interval is listed in Table.1. The coefficient α in the Shirahama sandstone was over 1.0 up to the confining pressure of 11 MPa, but, at higher confining pressure than that value, α dropped nearly to 0.7. At low confining pressure pore pressure effect on α was stronger than confining pressure effect, but the effect of confining pressure became larger than that of pore pressure at higher confining pressure. On the other hand, we determined α in Inada granite using another method similar to the cross-plotting method described by Walsh(1981). The coefficient of α in the Inada granite was determined by the following procedure. First, permeability K is plotted as a function of confining pressure at fixed values of pore pressure. These data are cross-plotted yielding Pc as a function of Pp for constant value of permeability. Then, we can directly determine the curves of constant K. Fig.3(a), (b), (c) show relation between permeability and modified effective confining pressure. Coefficient α in IGR, IGG, IGH are 0.86, 1.21, and 0.54, respectively. Our results agree with Bernabe's observation(1986) and Madden's proposition(1986) that transport properties of a crack network are not very sensitive to the anisotropy of the network.

Tensile strength and elastic wave velocities across three different rift, grain, hardway planes showed strong anisotropy. The anisotropy of the Inada granite were caused by the preexisting preferred orientation of microcracks and can be interpreted as the difference in crack density(Peng and Johnson 1972). As the cracks perpendicular to the macroscopic flow direction can not contributed as flow path, the permeability should be in the order of IGH, IGG, and IGR. However, in permeability measurement there appears no systematical anisotropy effect in the value of α . Only the preferred orientation of

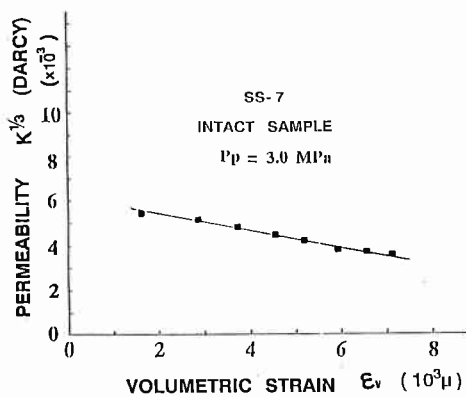


Fig.4 K versus volumetric strain for the Shirahama sandstone.

Table.1 The coefficient "alpha" in each pressure interval.

段階	A	B	C	D	E	F
α	1.05	1.29	1.55	0.77	0.79	0.72

microcracks does not characterize the fluid transport properties of granite, and that the same microcracks participate to the flow almost independently of each preferred orientation.

In the problem of fluid transport properties in fractured rocks, it is usual to assume that a natural fracture can be represented by a parallel plate. The following relationship between flow rate "q" and pressure gradient "dp/dx" is well known.

$$q = b^3 / 12\mu (dp/dx)$$

where b is the size of the fracture aperture and μ is the fluid viscosity. Fluid flow in a fracture is a rather sensitive function of aperture size. Thus, we investigated the correlation between permeability and volumetric strain under isotropic stress. In the Fig.4 data of experiment on the Shirahama sandstone are plotted on the diagram of cube root of permeability $K^{1/3}$ versus volumetric strain. All data points fall almost on a straight line. Krantz et al.(1979) and other investigators suggested that a flat plate model of the joint is inadequate, but, in our experiments indicate that a cubic law of permeability is almost adequate for sedimentary rocks with mostly unconnected porosity such as the Shirahama sandstone.

Fig.5 shows change of permeability with axial differential stress for the Shirahama sandstone. These measurements were made at 20 MPa of confining pressure and 12 MPa of pore pressure. At low axial stress, the permeability did not change. An increase of nearly threefold of permeability occurred prior to failure. Fig.6 shows a change of permeability with axial differential stress for IGR, IGG, IGH sample. At about a half of maximum axial stress, permeability decreased monotonically with increasing axial stress. This phenomenon is probably due to the closure of preexisting microcracks. At higher stress over a half of strength, permeability increased with increasing axial stress. These phenomena were observed in spite of different preexisting preferred orientations. This phenomenon is probably due to the occurrence of the stress induced microcracks. The variation in permeability with deformation is seen to be quite similar at each specimen of IGR, IGG, IGH with a decrease and increase of almost two orders of magnitude. The following relationship is used widely(Paterson 1983).

$$K = CR^2 \rho^m$$

where C is a numerical factor(probably around 0.3 to 0.4), R the hydraulic radius of the connected porosity, and ρ the porosity. m is close to 2 for a wide range of rocks with porosities varying from 0.1 % to 10 %(Brace et al. 1965). Here, we assume that ρ is defined as the dilatant volumetric strain in observed volumetric strain under deformation. In most of

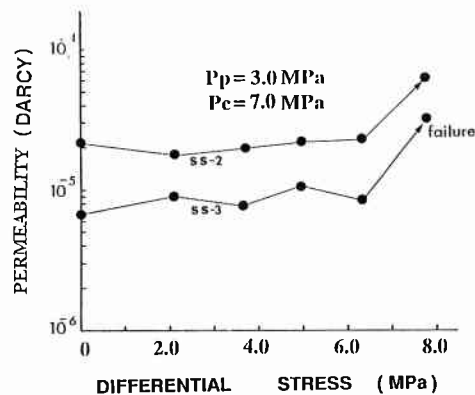


Fig.5 Permeability changes as a function of axial differential stress for the Shirahama sandstone.

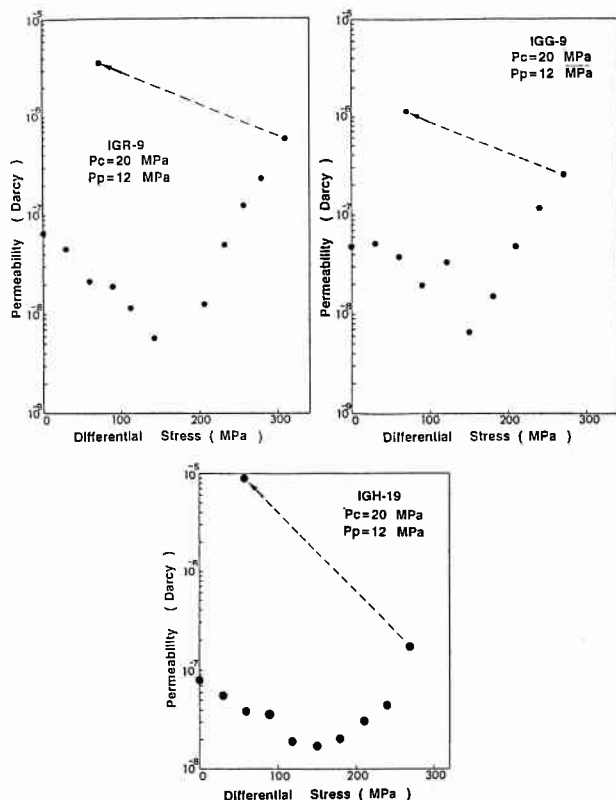


Fig.6 Permeability change as a function of axial differential stress for IGR, IGG, IGH specimens.

permeability measurement, the variation in K obtained must be due to change in porosity ρ (corresponding to dilatant volumetric strain). Because it is obviously shown that K decreased with increasing volumetric strain under hydrostatic pressure (Fig.4), and that K behaved synchronously with dilatant volumetric strain under axial loading (Fig.7). As CR^2 in previous equation is a factor characterizing the cross section of the equivalent channel in connection with its resistance to fluid flow, it can also interpret necessarily as difference on " CR^2 ". But, the effect on K was smaller by far than that on porosity ρ . Thus, we must recognize that ratio of dilatant volumetric strain to porosity at isotropic stress was different for different rocks and different preferred orientations. It is concluded that pore and crack aperture (corresponding to hydraulic radius) must be affected by hydrostatic and deviatoric stress. To discuss further in detail, we must measure electric conductivity and decide formation factor of each rock.

5. Conclusion

Permeability and volumetric strain were measured under confining pressure, pore pressure, and axial differential stress. The Shirahama sandstone cored perpendicular to bedding plane and Inada granite cored in mutually perpendicular directions were used in our experiments. The values of coefficient of α of the effective confining pressure $P_{eff} = P_c - \alpha P_p$ were calculated at each pressure. The values of α ranged between 0.7 and 1.5 for the Shirahama sandstone. Similarly, α for IGR, IGG, and IGH specimen were 0.86, 1.21, and 0.54, respectively. There was found no systematical anisotropy effect in the value of α for different preferred orientation of Inada granite. At initial axial stress, permeability decreased. With further increase in differential stress the sample become dilatant, and permeability correspondingly increased. As porosity and hydraulic radius are strongly affected by the stress, permeability difference in rocks and preferred orientations can be interpreted as the difference in each porosity and

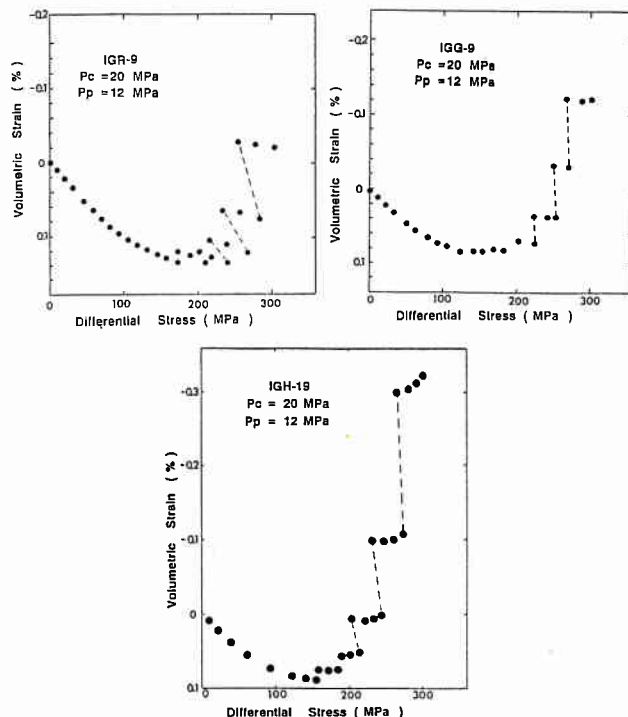


Fig.7 Axial differential stress versus volumetric strain curves for IGR, IGG, IGH specimens.

hydraulic aperture of microcracks.

The results of this study indicate that the stress-fluid pressure history influences the effective permeability of rocks, hence, the isolation performance of rock barrier around a repository of radioactive waste. The careful prediction of stress-fluid pressure change is necessary to assess the long-term safety of mined geologic disposal of high level radioactive waste.

References

- Bernabe, Y. 1986. The effective pressure law for permeability in Chelmsford granite and Barre granite. *Int. J. Rock Mech. Min. Sci.* 23: 267-275.
- Brace, W.F., J.B. Walsh, and W.T. Frangos 1968. Permeability of granite under high pressure. *J. Geophys. Res.* 73: 2225-2236.
- Brace, W.F. 1980. Permeability of crystalline and argillaceous rocks. *Int. J. Rock Mech. Min. Sci.* 17: 241-251.
- Kranz, R.L., A.D. Frankel, T. Engelder, C.H. Scholz. 1979. The permeability of whole and jointed Barre granite. *Int. J. Rock Mech. Min. Sci.* 16: 225-234.
- Kudo, Y., K. Hashimoto, O. Sano, K. Nakagawa. 1987. Relation between physical anisotropy and microstructures of granitic rock in Japan. *Proc 6th Congress on Rock Mech.* Montreal: 429-432.
- Mordecai, M. and L.H. Morris. 1971. An investigation into the changes of permeability occurring in a sandstone when failed under triaxial stress conditions. George B. Blar Ed. chapter 11. Port City Press.
- Paterson, M.S. 1983. The equivalent channel model for permeability and resistivity in fluid-saturated rock—a re-appraisal. *Mech Materials.* 2: 345-352.
- Peng, S. and A.M. Johnson. 1972. Crack growth and faulting in cylindrical specimens of Chelmsford granite. *Int. J. Rock Mech. Min. Sci.* 9: 37-86.
- Zoback, M.D. and J.D. Byerlee. 1975. The effect of microcrack dilatancy on the permeability of Westerly granite. *J. Geophys. Res.* 80: 752-755.
- Walsh, J.B. 1981. Effect of pore pressure and confining pressure on fracture permeability. *Int. J. Rock Mech. Min. Sci.* 18: 429-435.